

Efficient visible light detection using individual germanium nanowire field effect transistors

Y. H. Ahn

Division of Energy Systems Research, Ajou University, Suwon 443-749, Korea

Jiwoong Park^{a)}

The Rowland Institute at Harvard, Cambridge, Massachusetts, USA

(Received 29 July 2007; accepted 25 September 2007; published online 15 October 2007)

We report photoconductivity (PC) in individual germanium nanowire field effect transistors (GeFETs). PC measurements with a global illumination reveal that GeFETs can be used as a polarization-sensitive nanoscale light detector in the visible range. It is also found that the PC shows sensitive optical response especially in the low intensity regime. We observe a high internal gain in PC in conjunction with strong saturation behavior, which is attributed to the filling of surface trapping states. This mechanism for high internal gain is consistent with spatially resolved scanning photocurrent measurements, whose results confirm that optical absorption is in the linear regime.

© 2007 American Institute of Physics. [DOI: 10.1063/1.2799253]

Semiconducting nanowires (NWs) have been recently used as a core material in nanoscale optoelectronic components, including light-emitting diodes, waveguides, laser diodes, and various photodetectors.¹ In particular, individual NWs have been used in polarization-sensitive nanoscale light detectors for a wide range of semiconducting materials.²⁻⁸ It has been found for GaN (Ref. 8) and ZnO (Refs. 3 and 6) NWs that the presence of charge trapping states at the surface drastically affects the photoconductivity because of the high surface-to-volume ratio in NWs. In these wide-band-gap materials, the high internal gain mediated by the surface state is responsible for the dramatically enhanced photoresponse. Similar effect, on the other hand, has not been reported for visible range photodetectors.

Germanium (Ge) NWs have recently attracted interest for future electronic applications, due to their high carrier mobility and the relative ease of synthesis.⁹⁻¹² One of the major issues is the poor surface oxide properties of Ge and their influence on the electrical transport through NWs.¹³⁻¹⁶ While photoconductivity (PC) measurements on high-density arrays of Ge NWs have been recently reported,¹⁷ the optoelectronic properties of *individual* Ge NWs and the influence of surface states have not been reported before.

In this letter, we present PC measurements on individual Ge NWs in the visible range. Our Ge NW devices show a sensitive photoresponse due to the large absorption cross section and a high internal gain especially in the low light intensity regime. The PC shows a strong saturation behavior that is due to the surface state filling. In addition, scanning photocurrent measurements^{18,19} are performed for detailed studies on Ge NW photoresponse with spatial resolution.

Ge NWs are synthesized using a multistep, vapor-liquid-solid chemical vapor deposition technique reported earlier.¹¹ Au clusters (30 nm) were used as catalysts to grow Ge NWs at the total pressure of 500 Torr of 1.5% GeH₄ diluted in H₂. The nucleation and elongation temperatures were 320 and 280 °C, respectively. The NWs were then *p* doped with an exposure to B₂H₄ at 380 °C followed by a subsequent coating with *i*-Ge. For device fabrication, Ge NWs were first

suspended in methanol by a brief (~1 s) sonication and then deposited on an oxidized Si wafer substrate with a 220 nm thick thermal oxide layer that serves as a gate oxide. Both standard photo- and electron-beam lithography techniques followed by Ti metal evaporation and liftoff were used to define the source and drain electrodes to electrically contact Ge NWs (typically 50 nm in diameter), as shown schematically in Fig. 1(a). An atomic force microscopy (AFM) image of a representative Ge NW device is shown in Fig. 1(b).

Our Ge NW devices show standard field effect transistor operation with good Ohmic behavior of Ti contacts [inset of

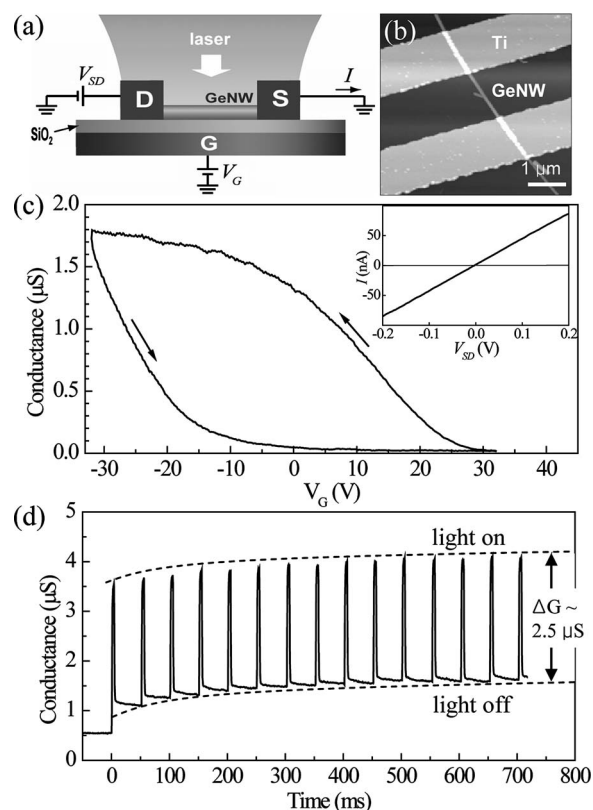


FIG. 1. (a) Schematic of the experimental setup. (b) AFM image of a Ge NW FET device. (c) dc conductance measured at $V_{SD}=0.1$ V. (d) A time trace of the device conductance while the laser beam is turned on and off repeatedly with a pulse duration of 5 ms ($V_{SD}=0.1$ V).

^{a)}Present address: Department of Chemistry and Chemical Biology, Cornell University, Ithaca, NY 14853. Electronic mail: jp275@cornell.edu

Fig. 1(c)]. Figure 1(c) shows a typical low-bias ($V_{SD}=0.1$ V) conductance versus gate voltage (V_G) curve measured under ambient conditions from one of our devices without light illumination. The large conductance at negative V_G corresponds to the p -type conduction of the Ge NW field effect transistor (FET). The gate sweep of the dc conductance exhibited a more pronounced hysteresis compared to other NWs such as Si NWs that we measured in similar device geometry. This extraordinary hysteresis in FETs with bare Ge NWs has been largely attributed to the high-density of charge trapping states on the surface. It has also been reported that the hysteresis can be dramatically reduced by proper passivation of Ge NW surfaces.^{13–15}

When individual Ge NW devices are illuminated with visible light ($\lambda=532$ nm), they show two distinctive time-dependent behaviors: a fast photoresponse with a large conductance increase and a slow PC component. Figure 1(d) shows the time trace of the conductance monitored at $V_{SD}=0.1$ V, while the laser light is turned on and off repeatedly (~ 10 kW/cm² and pulse duration=5 ms). Here, the whole active region of the device was illuminated. While the conductivity increases (drops) rapidly every time the light is turned on (off), the gradual increase of the dark signal (light off) is also observed as denoted by the dashed line.

While this slow background PC component displays a long relaxation time (decay time is ~ 10 s), the response time for the main PC component is fast, limited only by the shutter speed (~ 1 ms) of the system. The magnitude of the fast PC reaches the steady value of 2.5 μ S relative to the background signal.

The slow PC component with a long relaxation time is consistent with the results from the previous electrical transport measurements on Ge NWs, where the influence of the surface states has been investigated.¹⁵ The long relaxation time of the device conductance has been attributed to the conductance gain mediated by the slow dynamics of surface states (capture time in minutes). Here, the properties of the slow states are associated with the Ge oxide surface structure and the ambient environment.²⁰ The fast states (capture time in microseconds), on the other hand, are believed to be located at the interface between the Ge and the surrounding oxide layer. Both the fast and the slow surface states will contribute to the photoresponse observed in Ge NW, although the slow components could be suppressed by a proper passivation of the GeO_x surface.

In Fig. 2, we show the light intensity and the polarization dependence. Here, we are primarily concerned with the fast PC components by taking the average of the conductance change $\Delta G=(I_{\text{light}}-I_{\text{dark}})/V_{SD}$ extracted from similar measurements as in Fig. 1(d). First, the Ge NW PC is recorded for a wide range of light intensity of more than five orders of magnitude [Fig. 2(a)]. Surprisingly, we observe a significant PC signal even with an extremely low light intensity (<100 mW/cm²). Here, the Ge NW photoconductivity was explicitly compared to that of Si NW with similar dimensions, measured at the same experimental conditions. The PC for Ge NW is more than two orders of magnitude higher than that of Si, for instance, at 1 kW/cm² [denoted by an arrow in Fig. 2(a)]. Based on our measurements, we expect that this PC enhancement in Ge NWs will be even more pronounced at lower light intensity (three orders of magnitude higher than Si NW at 100 mW/cm²).

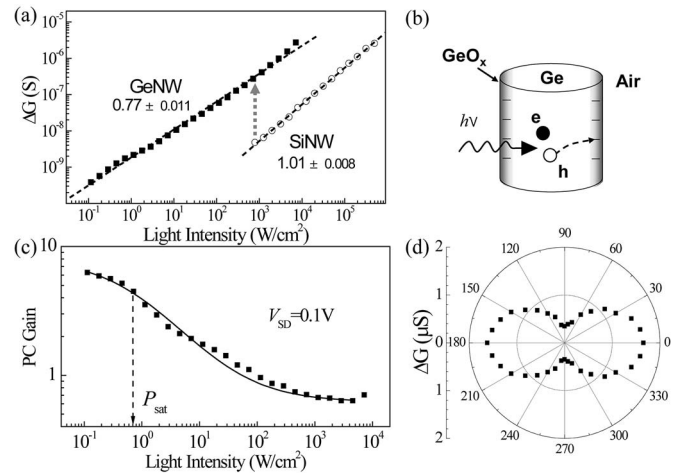


FIG. 2. (a) PC as a function of the light intensity for both Ge (filled rectangles) and Si (open circle, 30 nm in diameter) NWs with similar dimensions. Dashed lines are fit to the data. (b) Schematic of the internal gain mechanism. (c) PC gain vs light intensity for low-bias condition ($V_{SD}=0.1$ V). Solid line is fit to the data. (d) Polarization dependence of Ge NW PC.

The pronounced visible-range photoresponse can be largely attributed to the high photoconductivity gain originated from the charge trapping on the surface, a mechanism previously reported on the photoresponse of ZnO NW.^{3,6} When electron-hole pairs are generated upon light illumination, holes migrate to the surface while electrons drift out of the NW,^{15,20} resulting in an internal photoelectric gain [inset of Fig. 2(b)]. The density of accessible surface states decreases with increasing light intensity due to the surface state filling, and hence we see a decrease of the internal gain with increasing light intensity.⁶ The subunity exponent (slope=0.77) of Ge NW PC [Fig. 2(a)] is the manifestation of this gain saturation,³ and it is in striking contrast to the photoresponse of Si NWs that shows a linear power dependence.

Photoconductive gain (G_{PC}) can be expressed in terms of the observed photocurrent (I_{ph}) and the input power (P) as follows: $G_{PC}=(h\nu I_{ph})/(\eta e P)$, where η is the quantum efficiency, e is the electron charge, and $h\nu$ is a photon energy (2.33 eV). Shown in Fig. 2(c) is the plot of the gain as a function of the light intensity, deduced from the photocurrent measurements at low-bias conditions ($V_{SD}=0.1$ V). The decrease of the gain with increasing laser power reflects the gain saturation. The gain value was estimated to be around 6.4, for instance, at the light intensity of 110 mW/cm². This is a large value considering that only the fast component has been included in the calculations. Also, note that even higher gain will be obtained for high-bias conditions since the gain generally increases with increasing source-drain bias voltage.

Since the gain saturation is strongly related to the saturation of the surface states, our measurements can provide useful information about the surface state density. The plot of Fig. 2(c) was fitted by the power saturation curve,⁶ $G_{PC}=1/[1+(P/P_{\text{sat}})^n]$, where the saturation intensity of $P_{\text{sat}}=0.72$ W/cm² (absorbed photon amount of 2.4×10^8 s⁻¹) and $n=0.67$ have been deduced. This corresponds to the surface trap density of 1.6×10^{17} s⁻¹ cm⁻² for the Ge/GeO_x interface. If we consider the lifetime of the fast states (in microseconds) this is in good agreement with the reported surface charge density of 10^{11} cm⁻².²⁰

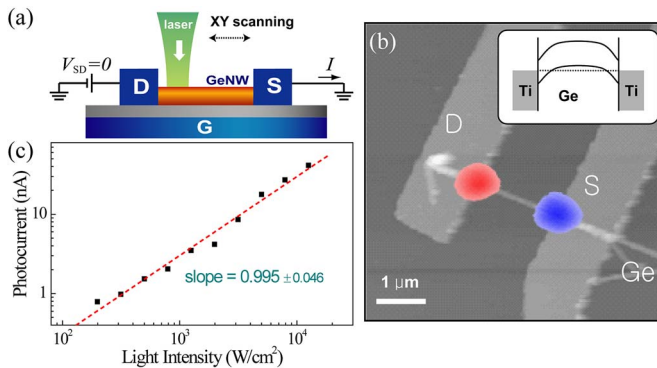


FIG. 3. (Color online) (a) Schematic of the scanning photocurrent (SPC) measurement setup. (b) SPC image (color), overlaid on an AFM image (gray) for a 2 μm long Ge NW at $V_G=V_{SD}=0$. (c) Magnitude of SPC (at drain electrode) as a function of the light intensity.

Ge has been largely considered as an efficient near-IR photodetector material. The results described above clearly demonstrate that our Ge NW devices are good photodetectors even in the visible range. In addition to the high conductivity gain, Ge NW has a larger quantum efficiency in the visible range when compared to SiNW (absorption depth is $\sim 1 \mu\text{m}$). This is due to the short penetration depth of Ge, which reaches down to 50 nm at 532 nm, for instance. This value matches the diameter of the Ge NWs measured in our experiments, and hence, the light absorption will be dramatically improved. As a result, our Ge NW devices become ultrasensitive photodetectors that are sensitive to the intensity of normal sunlight (roughly 100 mW/cm^2).

In Fig. 2(b), we show the polar plot of the PC versus the polarization of the incident light, which clearly shows that the NW conductance is the maximum (minimum) when the polarization of the incident light is parallel (perpendicular) to the axis of the NW. The PC anisotropy ratio $\sigma = (\Delta G_{\parallel} - \Delta G_{\perp}) / (\Delta G_{\parallel} + \Delta G_{\perp})$ of this device is 0.65. It shows that Ge NW devices are excellent polarization-sensitive light detectors with nanoscale spatial resolution. The observed PC anisotropy is most likely due to the anisotropy in the light absorption, which is caused by a large dielectric contrast between Ge NW and its surroundings.² Higher anisotropy ($\sigma > 0.9$) can be expected due to the large dielectric constants of Ge ($\epsilon = 16$), but the variation in light absorption would cause different internal gain for different polarization geometries, resulting in reduced PC anisotropy.

PC measurements with wide-field illumination in Figs. 1 and 2 offer information averaged over the whole length of the NW and cannot elucidate the local information of the photoinduced carriers within individual nanowires. In Fig. 3, we show a spatially resolved optical scanning measurement of the photocurrent. The experimental setup for a scanning photocurrent (SPC) measurements is similar to the one used in our previous report.¹⁸ A diffraction-limited laser beam (diameter of 500 nm at half maximum) was scanned to illuminate the NW devices, while the device conductance is recorded as a function of the position of the laser spot. The small spot size of the light enables us to record the photoinduced electronic signal that originates from the light illumination at different parts of Ge NWs.

In Fig. 3(b), the color scale represents the electrical current measured as a function of the laser position with the light intensity of 10 kW/cm^2 , when the bias $V_{SD}=0$ with an AFM image overlaid as a gray scale. The most striking fea-

ture in Fig. 3(b) is the localized current spots found near the drain electrode (positive: red) as well as near the source electrode (negative: blue). This can be explained from the energy band bending near the electrode contact, as discussed elsewhere.^{18,19} The electron band diagram of Ge NW FET can be extracted based on the observed photocurrent signal, and its gate dependent behavior is shown in the inset of Fig. 3(b).

The laser power dependence of the SPC provides information that is complimentary to the data shown in Figs. 1 and 2, since SPC at zero bias does not involve the gain mechanism. The SPC measured at the drain electrode is shown in Fig. 3(c) as a function of the light intensity. It clearly shows linear power dependence, in striking contrast to that of the PC shown in Fig. 2(a). This strongly indicates that the light absorption (proportional to SPC) in the Ge NW is in the linear response regime at this light intensity. This measurement also suggests that the saturation observed in PC is not caused by the decrease of light absorption inside the NW, but instead, is due to the internal gain saturation originating from the surface state filling.

In conclusion, we have shown that Ge NW can be an excellent candidate for polarization-sensitive nanoscale photodetectors especially in the visible range. The Ge NWs show extremely sensitive photoresponse especially at a low intensity regime, which is attributed to the internal gain mechanism, originating from the surface state filling. In the future, our research can be further extended to the studies of broad spectral response, effects of the surface passivation, and electron energy band profiles inside the Ge NW.

This work was mainly supported by the Rowland Junior Fellow program. Y.H.A. is also supported by the Nanoscopia Center of Excellence at Ajou University.

¹R. Agarwal and C. M. Lieber, *Appl. Phys. A: Mater. Sci. Process.* **85**, 209 (2006).

²J. F. Wang, M. S. Gudiksen, X. F. Duan, Y. Cui, and C. M. Lieber, *Science* **293**, 1455 (2001).

³H. Kind, H. Q. Yan, B. Messer, M. Law, and P. D. Yang, *Adv. Mater. (Weinheim, Ger.)* **14**, 158 (2002).

⁴Z. Y. Fan, P. C. Chang, J. G. Lu, E. C. Walter, R. M. Penner, C. H. Lin, and H. P. Lee, *Appl. Phys. Lett.* **85**, 6128 (2004).

⁵K. Keem, H. Kim, G. T. Kim, J. S. Lee, B. Min, K. Cho, M. Y. Sung, and S. Kim, *Appl. Phys. Lett.* **84**, 4376 (2004).

⁶C. Soci, A. Zhang, B. Xiang, S. A. Dayeh, D. P. R. Aplin, J. Park, X. Y. Bao, Y. H. Lo, and D. Wang, *Nano Lett.* **7**, 1003 (2007).

⁷S. Han, W. Jin, D. H. Zhang, T. Tang, C. Li, X. L. Liu, Z. Q. Liu, B. Lei, and C. W. Zhou, *Chem. Phys. Lett.* **389**, 176 (2004).

⁸R. Calarco, M. Marso, T. Richter, A. I. Aykanat, R. Meijers, A. V. Hart, T. Stoica, and H. Luth, *Nano Lett.* **5**, 981 (2005).

⁹L. J. Lauhon, M. S. Gudiksen, C. L. Wang, and C. M. Lieber, *Nature (London)* **420**, 57 (2002).

¹⁰D. W. Wang, Q. Wang, A. Javey, R. Tu, H. J. Dai, H. Kim, P. C. McIntyre, T. Krishnamohan, and K. C. Saraswat, *Appl. Phys. Lett.* **83**, 2432 (2003).

¹¹A. B. Greytak, L. J. Lauhon, M. S. Gudiksen, and C. M. Lieber, *Appl. Phys. Lett.* **84**, 4176 (2004).

¹²D. Wang and H. Dai, *Appl. Phys. A: Mater. Sci. Process.* **85**, 217 (2006).

¹³D. W. Wang, Y. L. Chang, Q. Wang, J. Cao, D. B. Farmer, R. G. Gordon, and H. J. Dai, *J. Am. Chem. Soc.* **126**, 11602 (2004).

¹⁴T. Hanrath and B. A. Korgel, *J. Am. Chem. Soc.* **126**, 15466 (2004).

¹⁵T. Hanrath and B. A. Korgel, *J. Phys. Chem. B* **109**, 5518 (2005).

¹⁶B. Yoo, A. Dodabalapur, D. C. Lee, T. Hanrath, and B. A. Korgel, *Appl. Phys. Lett.* **90**, (2007).

¹⁷B. Polyakov, B. Daly, J. Prikulis, V. Lissauskas, B. Vengalis, M. A. Morris, J. D. Holmes, and D. Erts, *Adv. Mater. (Weinheim, Ger.)* **18**, 1812 (2006).

¹⁸Y. Ahn, J. Dunning, and J. Park, *Nano Lett.* **5**, 1367 (2005).

¹⁹Y. Gu, E.-S. Kwak, J. L. Lensch, J. E. Allen, T. W. Odom, and L. J. Lauhon, *Appl. Phys. Lett.* **87**, 043111 (2005).

²⁰R. H. Kinston, *J. Appl. Phys.* **27**, 101 (1956).